THE JOURNAL OF BIOLOGICAL CHEMISTRY VOL. 285, NO. 2, pp. 1147–1152, January 8, 2010

Enzymatic Activity Is Required for the *in Vivo* Functions of CARM1*

Received for publication, June 19, 2009, and in revised form, September 29, 2009 Published, JBC Papers in Press, November 5, 2009, DOI 10.1074/jbc.M109.035865

Daehoon Kim, Jaeho Lee, Donghang Cheng, Jia Li, Carla Carter, Ellen Richie, and Mark T. Bedford[1]

From Science Park-Research Division, The University of Texas M. D. Anderson Cancer Center, Smithville, Texas 78957

CARM1 is one of nine protein arginine methyltransferases that methylate arginine residues in proteins. CARM1 is recruited by many different transcription factors as a positive regulator. Gene targeting of CARM1 in mice has been performed, and knock-out mice, which are smaller than their wild-type littermates, die just after birth. It has been proposed that CARM1 has functions that are independent of its enzymatic activity. Indeed, CARM1 is found to interact with a number of proteins and may have a scaffolding function in this context. However, CARM1 methylates histone H3, PABP1, AIB1, and a number of splicing factors, which strongly suggests that its impact on transcription and splicing is primarily through its ability to modify these substrates. To unequivocally establish the importance of CARM1 enzymatic activity *in vivo*, we generated an enzyme-dead knock-in of this protein arginine methyltransferase. We determined that knock-in cells and mice have defects similar to those seen in their knock-out counterparts with respect to the time of embryo lethality, T cell development, adipocyte differentiation, and transcriptional coactivator activity. CARM1 requires its enzymatic activity for all of its known cellular functions. Thus, small molecule inhibitors of CARM1 will incapacitate all of the enzyme's cellular functions.

There are nine mammalian protein arginine methyltransferases (PRMT1–9) (1). All of these enzymes have a common set of four conserved sequence motifs (I, post-I, II, and III) that, together with a THW loop, are involved in an active binding pocket. Outside of this conserved catalytic core, some of the PRMTs[2] harbor function domains such as an SH3 (Src homology 3) domain, tetratricopeptide repeats, and a zinc finger motif, which likely recognize substrate proteins or members of a protein complex that regulate their activity. The PRMTs catalyze the addition of methyl groups to the guanidine nitrogen atoms of arginine, which can both positively and negatively regulate protein-protein interactions (2–4). Arginine methylation is an abundant post-translational modification that regulates a diverse array of cellular functions (1).

CARM1 (coactivator-associated arginine methyltransferase 1) was the first PRMT to be identified as a transcriptional regulator (5). It methylates a number of proteins that are involved in transcription and RNA processing, including histone H3, AIB1, p300/CBP, PABP1 (poly(A)-binding protein 1), and CA150 (1). CARM1 knock-out mice die at birth and display defective T cell development, lung development, and adipogenesis (5–8). Cells derived from CARM1 knock-out embryos have impaired estrogen receptor-, c-Fos-, peroxisome proliferator-activated receptor γ-, and NF-κB-regulated transcription (7–10) and defects in the late stages of myogenic differentiation (11). Thus, CARM1 functions as a rather general transcriptional coactivator, much like p300/CBP.

In the phosphorylation field, the importance of the catalytic activity of enzymes has been investigated through the generation of kinase-dead knock-in mice. In some instances, these knock-ins phenocopy the traditional knock-out (12), and in others, there are clear distinctions between the enzyme-dependent phenotype and the scaffolding-dependent phenotype (13). In the acetyltransferase field, knock-ins of the p300/CBP coactivators have revealed nonredundant roles for their protein-binding KIX domains (14). In addition, the GCN5 knock-in mouse model has also exposed critical nonenzymatic functions for this protein; the knock-out mice die at E10.5, whereas the knock-in mice die as late as E16.5 (15).

Supporting a possible scaffolding role for CARM1 is the fact that it is a component of the nucleosomal methylation activator complex (16). CARM1 also interacts with a number of other transcriptional regulators, including the p160 family of coactivators (5), the transcriptional coactivator SRCAP (17), the coactivator Flightless I (Fli-1) (18), the Wnt signaling molecule β-catenin (19), the NF-κB subunit p65 (9), and the muscle regulatory factors Mef2D and Myog (11). Furthermore, in a number of instances, the enzyme-dead form of CARM1 retains partial coactivator activity in luciferase reporter assays: mutant CARM1 has partial activity with (*a*) an estrogen-response element (18), (*b*) a murine mammary tumor virus promoter (19), and (*c*) *MIP-2* and *IP-10* promoters (9). However, partial coactivator activity for mutant CARM1 was not seen on the *CCNE1* promoter (20).

The reporter assay studies are somewhat flawed because they use overexpression systems and the reporters are not fully chromatinized, like nuclear DNA. Thus, to address this issue of how critical the enzymatic activity of CARM1 is for its biological roles, we have generated an enzyme-dead CARM1 knock-in mouse model.

* This work was supported, in whole or in part, by National Institutes of Health Grant ES07784 from NIEHS (to institutional core facilities) and National Institutes of Health Grant CA016672 from NCI (to the Genetically Engineered Mouse Facility).

[1] Supported by National Institutes of Health Grant DK62248. To whom correspondence should be addressed. Tel.: 512-237-9539; Fax: 512-237-2475; E-mail: mtbedford@mdanderson.org.

[2] The abbreviations used are: PRMT, protein arginine methyltransferase; CBP, cAMP-response element-binding protein; E, embryonic day; GST, glutathione *S*-transferase; ES, embryonic stem; MEF, mouse embryonic fibroblast; PBS, phosphate-buffered saline.

EXPERIMENTAL PROCEDURES

Knock-in Vector Construction and Site-directed Mutagenesis—We previously generated a CARM1 knock-out vector (8). Using this vector, we introduced a point mutation at position 169, changing an arginine residue to an alanine. This was then used as our CARM1 knock-in vector. Site-directed mutagenesis was performed on GST-CARM1 and the original knock-out construct by PCR using mutant primer sets and the QuikChange XL kit (Stratagene).

Gene Targeting, Embryonic Stem Cell Culture, and Generation of CARM1 Mice—TC-1 ES cells were electroporated with PvuI-linearized pKI-CARM1 and selected in G418 (21). Genomic DNA from 40 neomycin-resistant colonies was screened for homologous recombination by BamHI digestion and Southern blot hybridization with an external probe. Seven clones were found to be correctly targeted. High-grade chimeric mice have been made successfully with the ES cell line A2. Males with a high contribution of ES cells were crossed with Black Swiss females to generate agouti F1 hybrids, thus demonstrating that the manipulated ES cells had undergone germ line transmission. We then crossed these heterozygous mice with the ubiquitous Flp recombinase-expressing "flipper" mouse (22) to obtain heterozygous mice that have lost their *Neo* cassette and are re-expressing enzyme-dead CARM1. For timed pregnancies, $CARM1^{KI/+}$ mice were mated overnight. Females were inspected for vaginal plugs the following morning, and noon was taken as day 0.5 of gestation (E0.5).

CARM1 Knock-in MEF Generation—Individual embryos from $CARM1^{KI/+}$ intercrosses at E14.5 were placed into culture as described (23). Cells were maintained on a 3T3 culture protocol in which 10^6 cells were passed onto a gelatinized 10-cm dish every 3 days. Two stable lines (KI13 and KI26) were established in this fashion.

In Vitro Methylation Reactions Using Recombinant Enzyme—GST-CARM1, GST-CARM1(R169A), and GST-CARM1(Y173A) were expressed and purified as described previously (3). *In vitro* methylation reactions were performed in a final volume of 30 μl of PBS (pH 7.4). The reaction contained 0.5–1.0 μg of substrate (GST-PABP1) and 1 μg of recombinant GST-CARM1. All methylation reactions were carried out in the presence of 0.42 μM *S*-adenosyl-L-[*methyl*-^{3}H]methionine (79 Ci/mmol from a 7.5 μM stock solution; PerkinElmer Life Sciences). The reaction was incubated at 30 °C for 1 h and then subjected to fluorography by separation on SDS-polyacrylamide gel, transferred to a polyvinylidene difluoride membrane, treated with EN^{3}HANCE™ (PerkinElmer Life Sciences), and exposed to film overnight at −80 °C.

In Vitro Methylation Reactions Using Cell Line Lysates as an Enzyme Source—MEF lines were grown to 80% confluency on a 10-cm plate. Cells were washed with PBS and scraped off the plate into 500 μl of PBS (pH 7.4). Cells were lysed by sonication, and the supernatant was used as the enzyme source. *In vitro* methylation reactions were performed by adding the cell lysate to 1 μg of GST-PABP1 bound to glutathione beads in the presence of 2 μl of the methyl donor (79 Ci/mmol (1 Ci = 37 GBq) from a 12.6 μM stock solution; Amersham Biosciences). The reaction was incubated at 30 °C for 1 h, and then the beads were washed three times with PBS. The substrate-bound beads were suspended in protein running buffer and boiled, and the samples were separated on a 10% SDS-polyacrylamide gel, transferred to a polyvinylidene difluoride membrane, sprayed with EN^{3}HANCE, and exposed to film overnight.

Histological Analysis and Antibodies—Day 18.5 embryos with their abdomens perforated were fixed in formalin and embedded in paraffin wax. Embryos were sectioned at 3 μm and subjected to immunohistochemical localization of anti-CARM1 (1:20) and anti-H3R17me2a (1:100) antibodies (Millipore). Staining was performed using the EnVision system (DAKO), and the counterstain was hematoxylin.

SMN Tudor Domain Pulldown Assays—MEFs were lysed in 0.5 ml of mild lysis buffer (150 mM NaCl, 5 mM EDTA, 1% Triton X-100, and 10 mM Tris-HCl (pH 7.5)). Fifteen micrograms of GST-SMN(Tudor) was bound to beads and incubated with MEF cell extracts (10-cm plate) for 2.5 h at 4 °C. After five washes with lysis buffer, the beads were boiled in loading buffer, separated by SDS-PAGE, and transferred onto polyvinylidene difluoride membranes. Western analysis was performed with anti-CA150 antibodies (Bethyl Laboratories).

Luciferase Assays and Transient MEF Transfections—ERE-TK-Luc has a single vitellogenin estrogen-response element containing a basal herpes simplex virus thymidine kinase promoter linked to firefly luciferase (30). pT7E2 contains human estrogen receptor driven by the Rous sarcoma virus promoter (30). pCMV-Renilla has *Renilla* luciferase driven by a cytomegalovirus promoter (Promega). MEFs were maintained in Dulbecco's modified Eagle's medium supplemented with 10% fetal bovine serum. Approximately 20 h before transfection, cells were seeded into each well of 24-well culture dishes. The cells in each well were transfected with FuGENE 6 transfection reagent (Roche Applied Science) according to the manufacturer's protocol. For each transfection, 25 ng of pCMV-Renilla, 150 ng of estrogen receptor, and 250 ng of ERE-TK-Luc were used. After 4 h of transfection, the cells were washed twice with PBS and grown in phenol red-free Dulbecco's modified Eagle's medium supplemented with 5% charcoal-striped fetal bovine serum and treated with 20 nM estradiol (Sigma). After 42–44 h, the cells were washed twice with PBS and harvested to perform luciferase assay using the Dual Luciferase assay system (Promega).

Flow Cytometry—For three-color immunofluorescence analysis, cells in Hanks' balanced salt solution containing 1% bovine serum albumin and 0.1% sodium azide were incubated with directly conjugated or biotinylated antibodies on ice for 30 min, followed by three washes. Binding of biotinylated antibodies was detected with streptavidin conjugated to allophycocyanin. The cells were fixed in 1% paraformaldehyde before analysis. For determination of double-negative subsets, lineage-positive cells were gated out after staining with a mixture of biotinylated antibodies to lineage markers CD4 and CD8, as well as with phycoerythrin-conjugated anti-CD44 and fluorescein isothiocyanate-conjugated anti-CD25 antibodies (Pharmingen). Cells were analyzed with a Coulter Epics Elite flow cytometer and analyzed using Coulter Elite software.

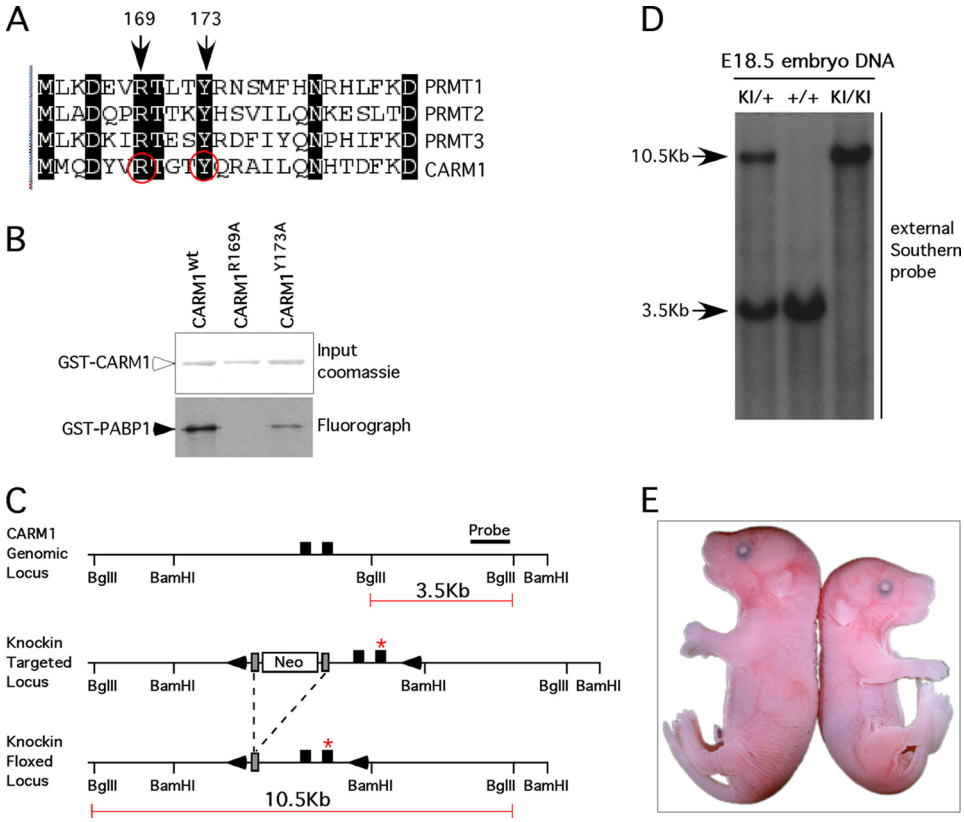

FIGURE 1. **Targeted knock-in of the *Carm1* gene.** *A*, a PRMT alignment in this region shows the degree of conservation within the region that was subjected to site-directed mutagenesis. Arg^{169} and Tyr^{173} (*circled* in *red*) were identified as potentially critical residues for CARM1 activity. *B*, site-directed mutagenesis was performed on Arg^{169} and Tyr^{173} in GST-CARM1, converting these amino acids to alanine. *In vitro* methylation reactions were then performed with the recombinant enzymes using GST-PABP1 as a substrate. *wt*, wild-type. *C*, the third exon of CARM1 (*) harbors a critical arginine residue (Arg^{169}) that was mutated to an alanine in the original knock-out construct to generate a knock-in construct. Heterozygous mice were crossed with a Flp recombinase-expressing mouse to remove the *Neo* cassette. *Arrowheads* depict *loxP* sites; *solid boxes* depict exons; and *gray boxes* depict *frt* sites. The position of the external Southern probe is noted. *D*, Southern blot analysis using BglII and an external probe shows the three different genotypes obtained from a heterozygous cross. *E*, knock-in day 18.5 embryos (on the *right*) are smaller than wild-type littermates.

RESULTS AND DISCUSSION

Generating the CARM1 Knock-in Mouse—To investigate the scaffolding *versus* enzymatic functions of CARM1, we generated an enzyme-dead knock-in CARM1 allele. We modified our original knock-out construct that has two floxed exons (exons 2 and 3) (8). These two exons encode a three-helix segment that is involved in *S*-adenosyl-L-methionine binding (cofactor) (24, 25). This region is highly conserved between PRMT family members (Fig. 1*A*). Within the context of a GST-CARM1 fusion, we tested the importance of two of these conserved residues (Arg^{169} and Tyr^{173}) for loss of *in vitro* methyltransferase activity. Alanine replacement of Arg^{169} generated a GST fusion with no enzymatic activity, whereas the conversion of Tyr^{173} to alanine resulted in a recombinant GST-CARM1 enzyme that still retained partial activity (Fig. 1*B*). Importantly, the conserved counterpart of Arg^{169} has been demonstrated, in both the PRMT1 and PRMT3 structures, to be a key residue for cofactor binding (26), and a detailed analysis of the CARM1 structure itself reveals that Arg^{169} hydrogen bonds to the *S*-adenosylhomocysteine molecule (27). Thus, there is a structural explanation for the effectiveness of the R169A mutation.

Next, the R169A mutation was engineered into the knock-out construct (Fig. 1*C*). We then generated targeted ES cells using this construct, which were identified by Southern blot hybridization. The ES cells were used to make chimeric mice, and the knock-in allele underwent germ line transmission. We then crossed these heterozygous mice, which still harbored the *Neo* cassette, to the ubiquitous Flp recombinase-expressing flipper mouse. This cross generated heterozygous mice that have lost their *Neo* cassette and are re-expressing enzyme-dead $CARM1^{KI/+}$ off one allele. We crossed these mice to generate homozygous knock-in ($CARM1^{KI/KI}$) embryos. The removal of the *Neo* cassette with Flp expression is expected to restore normal CARM1 levels, and that is indeed what we saw (Fig. 2*A*, *upper panel*). No $CARM1^{KI/KI}$ mice were detected at weaning, indicating that the loss of CARM1 activity causes recessive lethality. Embryos from $CARM1^{KI/+}$ intercrosses were analyzed by Southern blotting at E18.5 (Fig. 1*D*). During the cloning process, the BglII site was lost, and this is the site we use to facilitate the identification of wild-type and knock-in CARM1 alleles. $CARM1^{KI/KI}$ embryos were grossly normal but clearly smaller than their wild-type littermates (Fig. 1*E*). The $CARM1^{KI/KI}$ day 18.5 embryos looked very similar to the nullizygous CARM1 embryos of the same age (8).

$Carm1^{KI/KI}$ Embryos Produce Enzymatically Inactive CARM1—We then investigated the expression level and activity of the CARM1 knock-in protein in both embryos and MEF cell lines. CARM1 protein was expressed at normal levels in both day 18.5 embryos (Fig. 2*A*, *upper panel*) and MEFs derived from day 14.5 embryos (Fig. 2*A*, *middle panel*). As would be expected, no expression of CARM1 was seen in the knock-out counterparts.

Next, we used the MEF extracts as a source for methyltransferase activity to transfer a tritium-labeled methyl group from *S*-adenosyl-L-methionine onto a GST fusion protein harboring the CARM1 methylation motif of PABP1. Extracts from either $CARM1^{KI/KI}$ or $CARM1^{-/-}$ cells were unable to methylate GST-PABP1 (Fig. 2*A*, *lower panel*), demonstrating that CARM1 knock-in mice do indeed possess no CARM1 activity. Independent evidence of this was obtained from immunohistochemical experiments.

CARM1 functions as a homodimer (27), and to establish that the CARM1 R169A mutation results in a protein that can fold correctly, we transfected wild-type and knock-in MEFs with a

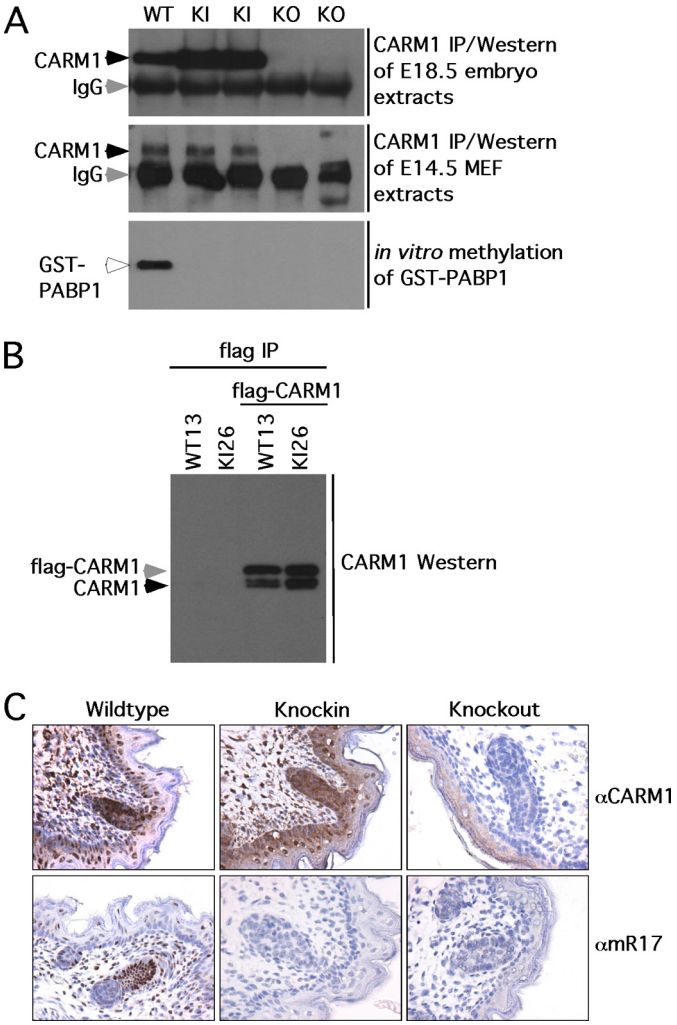

FIGURE 2. **CARM1 mutant R169A is expressed in embryos and MEFs but is inactive.** *A*, extracts were made from wild-type (*WT*), knock-in (*KI*), and knock-out (*KO*) day 18.5 mouse embryos. CARM1 was immunoprecipitated from these extracts and subjected to anti-CARM1 Western analysis (*upper panel*). MEF lines were generated from CARM1 wild-type, knock-in, and knock-out embryos. Immunoprecipitation (*IP*)/Western analysis showed CARM1 expression in wild-type and knock-in lines, but not in knock-out lines (*middle panel*). CARM1 wild-type cell lysates, but not knock-in cell lysates, have the ability to methylate GST-PABP1 *in vitro* (*lower panel*). *Black arrowheads* show the position of CARM1; the *white arrowhead* shows the position of GST-PABP1; and the *gray arrowheads* mark the IgG heavy chain. *B*, FLAG-tagged wild-type CARM1 can co-immunoprecipitate wild-type and mutant CARM1. CARM1 wild-type (13) and knock-in (26) MEF lines were transiently transfected with FLAG-CARM1, subjected to anti-FLAG immunoprecipitation, and immunoblotted with anti-CARM1 antibody. *C*, shown is the immunohistochemical localization of CARM1 and H3R17me2 in CARM1 wild-type, knock-out, and knock-in embryos. Similar sections of skin, with a hair follicle, are shown.

FLAG-CARM1 vector. After transfection, the tagged CARM1 was immunoprecipitated, and we performed Western blot analysis to determine whether the endogenous CARM1 (mutant or wild-type) could co-immunoprecipitate with the ectopically expressed protein. Both forms of CARM1 co-immunoprecipitated well with the tagged CARM1 (Fig. 2*B*), strongly suggesting that the CARM1 R169A mutation impairs the enzymatic activity of CARM1 but does not perturb its structure. The other scaffolding functions of CARM1 are thus also likely maintained.

CARM1 methylates the histone H3R17 site *in vitro* (28), and chromatin immunoprecipitation experiments have demonstrated that the recruitment of CARM1 to active promoters results in elevated H3R17me2 levels at these sites in cells (29, 30). Using immunohistochemical studies, we demonstrated that anti-CARM1 and anti-H3R17me2 immunoreactivity was widespread in the skin of wild-type day 18.5 embryos (Fig. 2*C*). In knock-in embryos, signal was observed with the anti-CARM1 antibody, but not with the anti-H3R17me2 antibody. In the skin from knock-out embryos, no signal was observed with either antibody.

CARM1 Knock-in Mice Display the Same Phenotype as Their Null Counterparts—Carm1$^{KI/+}$ mice are normal and fertile and were intercrossed to produce CARM1$^{KI/KI}$ mice. No homozygous knock-in mice were obtained at weaning (Fig. 3*A*). Further analysis revealed that homozygous knock-in pups died at birth, just like their knock-out counterparts (8). CARM1 functions as a homodimer (27), and one would expect to see a dominant-negative effect in CARM1$^{KI/+}$ mice because >50% of CARM1 activity would be lost in these heterozygous mice. However, we did not see a dominant-negative effect, and heterozygous knock-out and knock-in mice were born at the same frequency (Fig. 3*A*). This suggests that the expression levels of CARM1 are not limiting for its normal developmental functions, even when reduced to as much as 25% of its wild-type activity.

Serial analysis of gene expression of CARM1 wild-type and knock-out embryos revealed an important role for CARM1 in adipocyte differentiation, particularly brown fat development (7). One of the most dramatically differentially expressed genes was *THRSP* (thyroid hormone-responsive spot 14), which was reduced at least 5-fold in CARM1 knock-out embryos. Here, we compared the levels of THRSP protein expression in CARM1 wild-type, knock-out, and knock-in day 18.5 embryos. Western analysis revealed that THRSP protein was largely absent in both knock-in and knock-out embryo extracts (Fig. 3*B*). CARM1 knock-in embryos are thus defective in adipogenesis.

Next, we investigated the requirement of CARM1 activity for estrogen-dependent transcription. It has been shown that CARM1 action is critical for estradiol-stimulated gene expression (8, 31). We used a panel of MEF lines to determine the effect of CARM1 total loss (KO20) and CARM1 activity loss (KI26) on hormone-dependent activation of an estrogen receptor α-luciferase reporter construct (Fig. 3*C*). Reporter activity was much reduced in the absence of CARM1 protein and was reduced to a lesser degree in the absence of CARM1 activity. As reported before, it seems that in the context of a partially chromatinized reporter system, the enzyme-dead form of CARM1 does possess some transcriptional coactivator activity.

Finally, the CARM1 substrate CA150 complexes with the Tudor domain-containing protein SMN (3). Using knock-out MEF extracts, we have previously shown that this interaction requires the presence of CARM1. Here, we demonstrated that not only is the presence of CARM1 needed for this interaction to occur, but also its intact methyltransferase activity. Roughly equal amounts of CA150 were found in the different MEF lines (Fig. 3*D*, *lower panel*). In pulldown experiments, the Tudor domain of SMN was able to interact only with methylated CA150, derived from wild-type cells (Fig. 3*D*, *upper panel*).

A

	WT	Het	Total
KO	180(35%)	350(65%)	530
KI	91(31%)	206(69%)	297

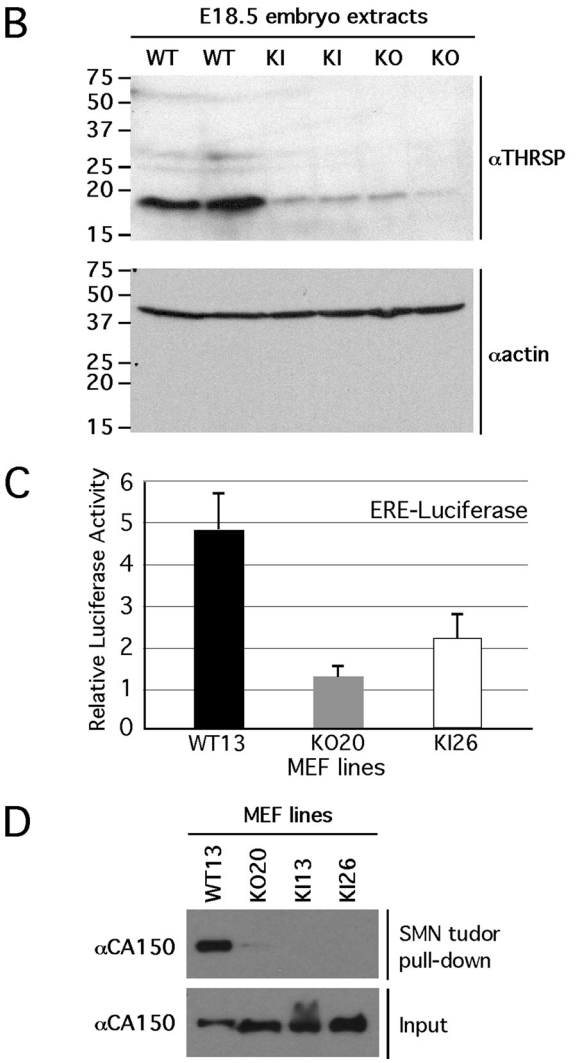

FIGURE 3. **CARM1 knock-in mice and cells display the same phenotypes as their knock-out counterparts.** *A*, genotypes of offspring from CARM1 knock-in (*KI*) and knock-out (*KO*) heterozygous (*Het*) crosses. The genotyping was performed after weaning. Genomic DNA was extracted and subjected to Southern blot analysis to determine the genotype. *Values* in *parentheses* indicate the percentage of each genotype. *B*, THRSP (spot 14) expression is reduced in both knock-out and knock-in day 18.5 embryo extracts. Western analysis was performed with an anti-THRSP antibody. An anti-actin Western blot served as a loading control. *C*, estrogen receptor-mediated transcription of a luciferase reporter is reduced in knock-out and knock-in MEF cells as opposed to wild-type (*WT*) cells. The S.D. is shown, and all changes are significant. *ERE*, estrogen-response element. *D*, the interaction between SMN and CA150 is dependent on CARM1 activity. A pulldown experiment was performed using GST-SMN(Tudor). Lysates from CARM1 wild-type (WT13), null (KO20), and knock-in (KI13 and KI26) MEF lines were subjected to this pulldown analysis and immunoblotted with anti-CA150 antibody. The input is shown in the *lower panel*.

This experiment shows that the CA150-SMN interaction is direct and not mediated by a potential scaffolding function of CARM1.

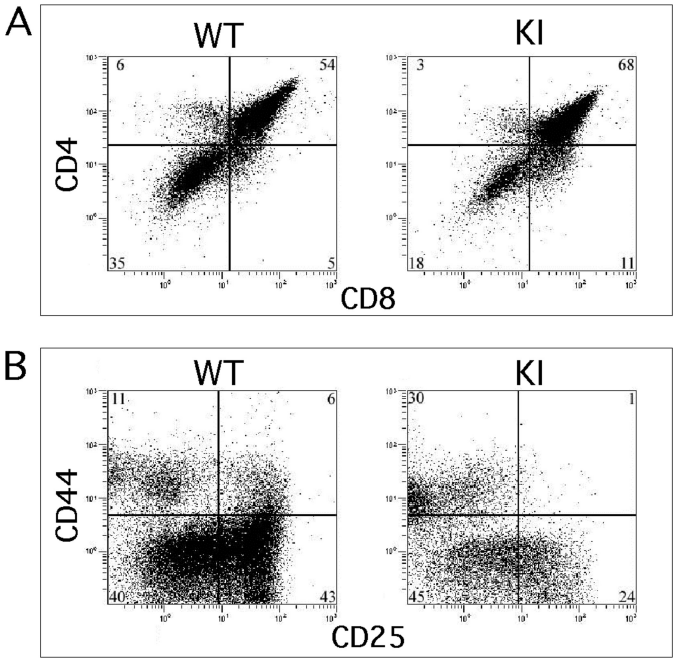

FIGURE 4. **CARM1 knock-in day 18.5 embryos display a partial thymocyte developmental arrest.** Shown are the results from flow cytometric analysis of thymocytes from CARM1 wild-type (*WT*) and knock-in (*KI*) day 18.5 mouse embryos for the expression of CD4 *versus* CD8 in the total thymocyte population (*A*) and CD44 *versus* CD25 in the gated double-negative compartment (*B*). The percentage of cells in each quadrant is reported.

CARM1 Knock-in Mice Have a T Cell Developmental Block—CARM1 protein is required for normal T cell development (6), but is its activity needed? To address this issue, flow cytometric analysis was performed on thymocyte subsets, and we found that thymocyte differentiation was indeed blocked at an early stage in CARM1$^{KI/KI}$ embryos. Fig. 4*A* shows a reduction in the percentage of CD4-CD8 double-negative thymocytes in CARM1 knock-in day 18.5 embryos compared with wild-type littermates. Moreover, analysis of double-negative subsets showed a marked developmental block at the DN1 ($CD44^+CD25^-$) progenitor stage (Fig. 4*B*). Like the knock-out (6), the knock-in thymuses also displayed a reduction in cellularity (~65%) (data not shown). Thus, loss of CARM1 enzymatic activity results in a block in early thymocyte maturation that phenocopies the developmental arrest previously reported for CARM1 knock-out embryos (6).

Here, we have demonstrated that CARM1 requires enzymatic activity for its *in vivo* functions. CARM1$^{KI/KI}$ and CARM1$^{-/-}$ day 18.5 embryos display the same adipocyte and T cell developmental defects (Figs. 3 and 4). These two mouse models also present with the same time of lethality: homozygous (knock-in and knock-out) mice are born alive but die before taking their first breath. Thus, on the whole systems level (*in vivo*), the integrity of CARM1 methyltransferase activity is critical. However, transcriptional reporter assay using cell lines derived from knock-out and knock-in embryos reveals that the enzyme-dead form of CARM1 does possess some residual coactivator activity (Fig. 3*C*). This lingering activity is clearly not sufficient to rescue any of the phenotypes we have analyzed to this point. We are currently undertaking a transcriptome analysis of knock-out *versus* knock-in MEFs to possibly identify

transcriptional pathways that do not require the enzymatic activity of CARM1. In addition, it is unlikely that all of the cellular functions of CARM1 have been identified, and in the future, these two mouse models can be used to evaluate the importance of CARM1 enzymatic activity within the context of each new functional discovery.

CARM1 levels have been found to be elevated in castration-resistant prostate cancer (32, 33), as well as in aggressive breast tumors that also express high levels of the oncogenic coactivator AIB1 (20). AIB1 functions as a scaffolding molecule that bridges nuclear receptors and CARM1/PRMT1 (34). Importantly, CARM1 methylates AIB1, thereby regulating its activity and stability (35, 36). The recruitment of CARM1 to estrogen receptor α-regulated promoters is dependent on the presence of AIB1, and CARM1 is essential for estrogen-induced proliferation of the MCF-7 breast cancer cell line (37). CARM1 is thus a good target for small molecule drug development. The study presented here provides evidence that specific and potent small molecule inhibitors will disable all of the reported functions of CARM1.

Acknowledgment—We thank Nancy Otto for immunohistochemistry.

REFERENCES

1. Bedford, M. T., and Clarke, S. G. (2009) *Mol. Cell* **33,** 1–13
2. Bedford, M. T., Frankel, A., Yaffe, M. B., Clarke, S., Leder, P., and Richard, S. (2000) *J. Biol. Chem.* **275,** 16030–16036
3. Cheng, D., Côté, J., Shaaban, S., and Bedford, M. T. (2007) *Mol. Cell* **25,** 71–83
4. Iberg, A. N., Espejo, A., Cheng, D., Kim, D., Michaud-Levesque, J., Richard, S., and Bedford, M. T. (2008) *J. Biol. Chem.* **283,** 3006–3010
5. Chen, D., Ma, H., Hong, H., Koh, S. S., Huang, S. M., Schurter, B. T., Aswad, D. W., and Stallcup, M. R. (1999) *Science* **284,** 2174–2177
6. Kim, J., Lee, J., Yadav, N., Wu, Q., Carter, C., Richard, S., Richie, E., and Bedford, M. T. (2004) *J. Biol. Chem.* **279,** 25339–25344
7. Yadav, N., Cheng, D., Richard, S., Morel, M., Iyer, V. R., Aldaz, C. M., and Bedford, M. T. (2008) *EMBO Rep.* **9,** 193–198
8. Yadav, N., Lee, J., Kim, J., Shen, J., Hu, M. C., Aldaz, C. M., and Bedford, M. T. (2003) *Proc. Natl. Acad. Sci. U.S.A.* **100,** 6464–6468
9. Covic, M., Hassa, P. O., Saccani, S., Buerki, C., Meier, N. I., Lombardi, C., Imhof, R., Bedford, M. T., Natoli, G., and Hottiger, M. O. (2005) *EMBO J.* **24,** 85–96
10. Fauquier, L., Duboé, C., Joré, C., Trouche, D., and Vandel, L. (2008) *FASEB J.* **22,** 3337–3347
11. Dacwag, C. S., Bedford, M. T., Sif, S., and Imbalzano, A. N. (2009) *Mol. Cell. Biol.* **29,** 1909–1921
12. Chan, R., Hardy, W. R., Laing, M. A., Hardy, S. E., and Muller, W. J. (2002) *Mol. Cell. Biol.* **22,** 1073–1078
13. Kullander, K., Mather, N. K., Diella, F., Dottori, M., Boyd, A. W., and Klein, R. (2001) *Neuron* **29,** 73–84
14. Kasper, L. H., Boussouar, F., Ney, P. A., Jackson, C. W., Rehg, J., van Deursen, J. M., and Brindle, P. K. (2002) *Nature* **419,** 738–743
15. Bu, P., Evrard, Y. A., Lozano, G., and Dent, S. Y. (2007) *Mol. Cell. Biol.* **27,** 3405–3416
16. Xu, W., Cho, H., Kadam, S., Banayo, E. M., Anderson, S., Yates, J. R., 3rd, Emerson, B. M., and Evans, R. M. (2004) *Genes Dev.* **18,** 144–156
17. Monroy, M. A., Schott, N. M., Cox, L., Chen, J. D., Ruh, M., and Chrivia, J. C. (2003) *Mol. Endocrinol.* **17,** 2519–2528
18. Lee, Y. H., Campbell, H. D., and Stallcup, M. R. (2004) *Mol. Cell. Biol.* **24,** 2103–2117
19. Koh, S. S., Li, H., Lee, Y. H., Widelitz, R. B., Chuong, C. M., and Stallcup, M. R. (2002) *J. Biol. Chem.* **277,** 26031–26035
20. El Messaoudi, S., Fabbrizio, E., Rodriguez, C., Chuchana, P., Fauquier, L., Cheng, D., Theillet, C., Vandel, L., Bedford, M. T., and Sardet, C. (2006) *Proc. Natl. Acad. Sci. U.S.A.* **103,** 13351–13356
21. Deng, C., Wynshaw-Boris, A., Zhou, F., Kuo, A., and Leder, P. (1996) *Cell* **84,** 911–921
22. Farley, F. W., Soriano, P., Steffen, L. S., and Dymecki, S. M. (2000) *Genesis* **28,** 106–110
23. Weiss, R. S., Enoch, T., and Leder, P. (2000) *Genes Dev.* **14,** 1886–1898
24. Weiss, V. H., McBride, A. E., Soriano, M. A., Filman, D. J., Silver, P. A., and Hogle, J. M. (2000) *Nat. Struct. Biol.* **7,** 1165–1171
25. Zhang, X., Zhou, L., and Cheng, X. (2000) *EMBO J.* **19,** 3509–3519
26. Zhang, X., and Cheng, X. (2003) *Structure* **11,** 509–520
27. Yue, W. W., Hassler, M., Roe, S. M., Thompson-Vale, V., and Pearl, L. H. (2007) *EMBO J.* **26,** 4402–4412
28. Schurter, B. T., Koh, S. S., Chen, D., Bunick, G. J., Harp, J. M., Hanson, B. L., Henschen-Edman, A., Mackay, D. R., Stallcup, M. R., and Aswad, D. W. (2001) *Biochemistry* **40,** 5747–5756
29. An, W., Kim, J., and Roeder, R. G. (2004) *Cell* **117,** 735–748
30. Kleinschmidt, M. A., Streubel, G., Samans, B., Krause, M., and Bauer, U. M. (2008) *Nucleic Acids Res.* **36,** 3202–3213
31. Lupien, M., Eeckhoute, J., Meyer, C. A., Krum, S. A., Rhodes, D. R., Liu, X. S., and Brown, M. (2009) *Mol. Cell. Biol.* **29,** 3413–3423
32. Hong, H., Kao, C., Jeng, M. H., Eble, J. N., Koch, M. O., Gardner, T. A., Zhang, S., Li, L., Pan, C. X., Hu, Z., MacLennan, G. T., and Cheng, L. (2004) *Cancer* **101,** 83–89
33. Majumder, S., Liu, Y., Ford, O. H., 3rd, Mohler, J. L., and Whang, Y. E. (2006) *Prostate* **66,** 1292–1301
34. Koh, S. S., Chen, D., Lee, Y. H., and Stallcup, M. R. (2001) *J. Biol. Chem.* **276,** 1089–1098
35. Feng, Q., Yi, P., Wong, J., and O'Malley, B. W. (2006) *Mol. Cell. Biol.* **26,** 7846–7857
36. Naeem, H., Cheng, D., Zhao, Q., Underhill, C., Tini, M., Bedford, M. T., and Torchia, J. (2007) *Mol. Cell. Biol.* **27,** 120–134
37. Frietze, S., Lupien, M., Silver, P. A., and Brown, M. (2008) *Cancer Res.* **68,** 301–306